Optical Engineering

OpticalEngineering.SPIEDigitalLibrary.org

Analysis of image motion on autofocus precision for aerial cameras

Fanhao Meng
Yalin Ding
Dejiang Wang
Jihong Xiu

SPIE.

Analysis of image motion on autofocus precision for aerial cameras

Fanhao Meng,[a,b,c,*] Yalin Ding,[a,c] Dejiang Wang,[a,c] and Jihong Xiu[a,c]
[a]Chinese Academy of Sciences, Changchun Institute of Optics, Fine Mechanics and Physics, Changchun, Jilin 130033, China
[b]University of Chinese Academy of Sciences, Beijing 100049, China
[c]Chinese Academy of Sciences, Key Laboratory of Airborne Optical Imaging and Measurement, Changchun, Jilin 130033, China

Abstract. Aerial cameras often suffer from image motion due to the severe aerial environments that decrease the autofocus precision. An analysis of the influence of image motion on autofocus precision is provided to obtain the optimal focus position. First, the focus measure function based on discrete Fourier transform is applied to evaluate the sharpness of the collected image for autofocusing. Then, two forms of image motion model, including linear shift and jitter, are discussed and analyzed. Finally, a quadratic fitting curve is employed on the focus measure function for image sequence. The maximum of the fitted curve corresponds to the optimal focus position. Experimental results demonstrate that the maximum value of the focus measure function decreases more than 10% approximately when the image motion increases to five pixels, and the optimal focus position computed by quadratic fitted curve generated a good performance in autofocus techniques. The proposed autofocus algorithm can be applied to aerial cameras. [DOI: 10.1117/1.OE.54.8.083102]

Keywords: aerial camera; autofocus; image motion; linear shift motion; jitter motion; quadratic fitting.

Paper 150538 received Apr. 26, 2015; accepted for publication Jul. 2, 2015; published online Aug. 7, 2015.

1 Introduction

Aerial cameras often suffer from image motion due to the variation of temperature and atmosphere pressure, which severely decreases the resolution and the quality of images. Consequently, it is essential to equip aerial cameras with autofocus systems to improve image quality.

In the past decades, many autofocus methods have been proposed in the extensive literature.[1–10] The image-based passive autofocus algorithms are widely studied for their high accuracy and no requirement for extra equipment.[11–13] These techniques, in general, adjust the distance between the sensor and the lens to realize autofocus using the image sharpness measure functions without user intervention.[12] In these passive approaches, the sharpness measure functions evaluate the degree of infocus of the image collected at various focus locations, and the optimal focus position is obtained at the position where the sharpness measure function is maximized.[13]

The image motion plays an important role in the autofocusing system, which occurs when relative motion exists between the sensor and the object during the exposure time.[14] The existence of image motion decreases the definition of the image and affects the image's interpretability. Even though aerial cameras are equipped with autofocus and motion compensation systems, several other factors including airborne platform vibration and air turbulence can still lead to unsatisfactory image quality.

From the existing literature, almost all autofocus approaches discussed were based on sharp images or images without motions.[3–10] To date, there has been no theoretical investigation of the relationship between image motion and autofocus techniques. Therefore, it is necessary and crucial to analyze these influences. In this paper, we carry out the analysis of influence of motions on autofocus precision for the first time. Passive autofocus approaches based on image sequences with motion are proposed, and the precision of autofocus is analyzed. Moreover, a method based on quadratic fitting is proposed in this paper; it can optimize the autofocus approaches of image sequences with motions of aerial cameras.

The remainder of this paper is organized as follows. Section 2 describes the model of frequency-based sharpness measure function and discusses the influence of linear shift motion and jitter motion on focus measure function. Section 3 gives a theoretical sensitivity analysis of motion on autofocus precision. Experimental results are demonstrated and compared in Sec. 4. Section 5 summarizes the results of this analysis.

2 Influence of Motion on Focus Measure Function

2.1 *Model of Sharpness Focus Measure*

In addition to some well-known sharpness measure functions,[9,15] frequency-based focus measures have been proposed in recent years.[8,13,16] They transform the image from spatial domain into frequency domain via a Fourier transform or a wavelet transform.[10,16] Then, the focus measure is calculated by computing the transformed coefficients or their distributions. The amplitudes of the high-frequency components are summed as a sharpness focus measure.[12] In general, the more sharp edges or details an image has, the more high-frequency components the frequency spectrum carries. Fig. 1 shows the images of Lena with and without motions and their Fourier frequency spectra. Comparing the

*Address all correspondence to: Fanhao Meng, E-mail: mengfanhao89@126.com

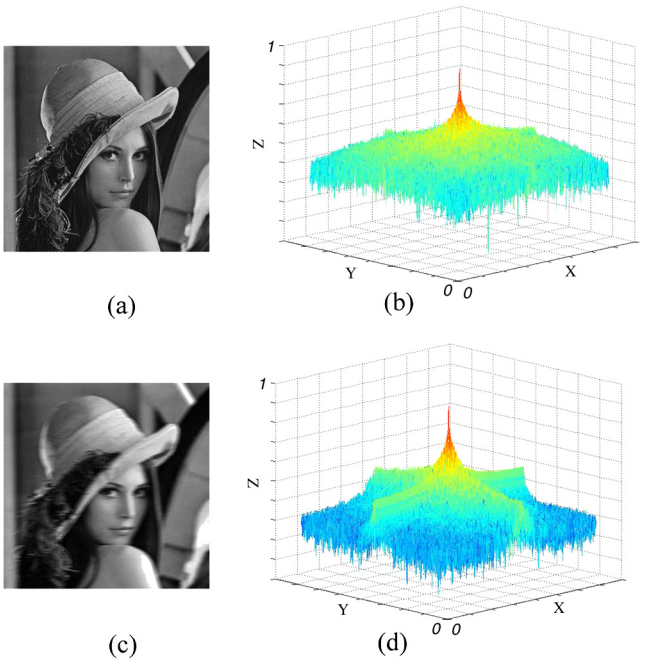

Fig. 1 Frequency spectrum of image: (a) Lena, (b) frequency spectrum of Lena, (c) Lena with motions, and (d) frequency spectrum of Lena with motions.

frequency spectrum of two images, it is obvious that the image with motion has less high-frequency components. It has been presented that the frequency-based focus measure is robust with noise and has comparable precision to some existing well-known sharpness measure functions.[17]

First, we let $y(i,j)$ denote the intensity of pixel (i,j) in an image of size $M \times N$. Then, the calculation of the focus measure of frequency spectra-based function F_{DFT} is described using the discrete Fourier transform (DFT) as follows:

$$F_{\mathrm{DFT}} = \sum_{u}\sum_{v} Y(u,v) = \sum_{i=1}^{M}\sum_{j=1}^{N} |\mathrm{DFT}\{y(i,j)\}|, \tag{1}$$

where (u,v) are the components of frequency.

2.2 *Influence of Linear Shift on Focus Measure Function*

Linear shift is the simplest model of image motion. It occurs when relative motion exists between the image sensor and the object at a constant velocity and along one direction in the $x-y$ plane during the exposure time.[18] If the relative motion exists in the direction of the x axis at a constant velocity of v, then the relative motion l between the image sensor and the object over the exposure time t_{exp} can be described by

$$l = v \times t_{\mathrm{exp}}. \tag{2}$$

In this section, the relative motion between the image sensor and the object is limited in the $x-y$ plane. It should be noted that motion along the z axis also exists, which can affect the focus if not properly controlled.[14] Given that the flight height of aerial cameras is much larger than the focus length, motion in the z axis direction is so tiny that its influence could be ignored.

The linear shift is a directional blur and will affect the image differently based on the direction, i.e., lines and edges that are along the direction of the motion will not blur. So the information that along the motion direction will not be affected. Thus, the blurring image with linear shift motion is modeled as a convolution with a one-dimensional rectangle function in the direction of the motion.[14,19] The width of the rectangle function is relative to the distance of the linear shift, therefore

$$g_{\mathrm{motion}}(i,j) = y(i,j) * \mathrm{rect}\left(\frac{x}{l}\right), \tag{3}$$

where * indicates the convolution operator. The rectangle function along the direction of the x axis is given by

$$\mathrm{rect}\left(\frac{x}{l}\right) = \begin{cases} 1 & |x| < l/2 \\ 1/2 & |x| = l/2 \\ 0 & |x| > l/2 \end{cases}. \tag{4}$$

For an image with linear shift motion, the DFT of the image can be described as

$$G_{\mathrm{motion}}(u,v) = Y(u,v) \cdot \mathrm{sinc}(l \cdot u). \tag{5}$$

The Fourier transfer function of rectangle function is sinc function, that is

$$\mathrm{DFT}\left[\mathrm{rect}\left(\frac{x}{l}\right)\right] = \mathrm{sinc}(l \cdot u) = \frac{\sin(\pi \cdot l \cdot u)}{(\pi \cdot l \cdot u)}. \tag{6}$$

According to Eq. (5), the Fourier transform function of the image with linear motion is contaminated with $\mathrm{sinc}(l \cdot u)$. The sinc function has lower amplitude when the frequency components are in higher interval of frequency. Fig. 2 illustrates the Fourier transform of the sinc functions with l equal to 1, 2, 4, and 8 pixels, respectively.

According to Eq. (1), the frequency spectra-based focus measure of an image is the sum of the amplitudes of the high-frequency components. In other words, the focus measure is the integration of the high-frequency components in the frequency spectrum. The area below the spectrum curve represents the focus measure, as shown in Fig. 3. The curve of the frequency spectrum gets closer to zero when the image motion increases.

The frequency spectra of different images are different in the domain of high-frequency components. The sinc function has the characteristic of a low-pass filter. As the image motion proceeds, high-frequency components are attenuated. When we utilize motion images for autofocusing, the weight of frequency components has different distribution in comparison to that of images without motions. If the images carry the same amount of motions, then the influence of motions affected by sinc functions is the same for all the images. The motion will decrease the maximum of focus measure, but the peak of focus measure function will not be changed. The position of the peak in the focus measure curve can still correctly reflect the optimal focus position.

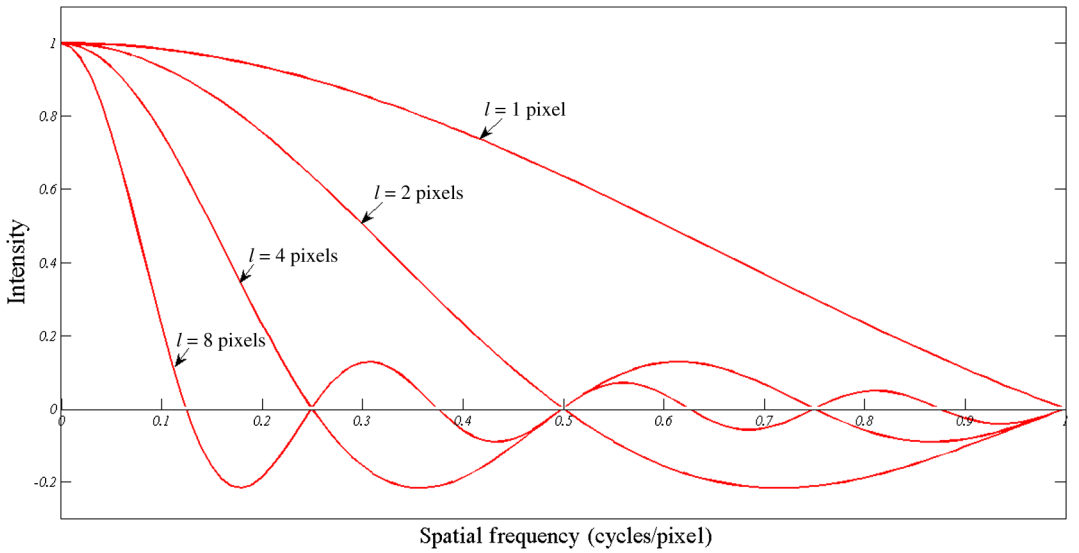

Fig. 2 Sinc functions with l equal to 1, 2, 4, and 8 pixels, respectively.

2.3 *Influence of Jitter Motion on Focus Measure Function*

Jitter is another model of image motion, which occurs when relative motion exists between the image sensor and the object while randomly changing direction at fast rate in all directions compared to the exposure time. Unlike the linear shift motion in one direction that causes directional smear, the jitter motion will result in image blur in all directions.

Jitter motion can be modeled as the convolution of an image with a Gaussian function.[14,19] That is

$$g_{\text{jitter}}(i,j) = h_{\text{jitter}}(i,j) * y(i,j) = \left(\frac{1}{\sqrt{2\pi}\sigma} e^{\frac{-(i^2+j^2)}{2\sigma^2}}\right) * y(i,j), \tag{7}$$

where σ is the standard deviation of the motion.

When autofocusing via images with jitter motion, the sharpness measure function is affected by the blurring of jitter. To develop a simple model for analysis, we simplify the result of Fourier transform and consider the components of frequency spectrum in 1-D; then the Fourier transform of the image with jitter motion can be described as

$$G_{\text{jitter}}(u) = H_{\text{jitter}}(u) \cdot Y_{\text{jitter}}(u), \tag{8}$$

where

$$H_{\text{jitter}}(u) = \text{DFT}(h_{\text{jitter}}) = e^{-2(\pi\sigma u)^2}. \tag{9}$$

The frequency spectrum components of an image with jitter motion are the same as that without motion. However, the weights of different components are changed by the effect of Gaussian function. Fig. 4 illustrates the Gaussian function with the impact of various amounts of jitter in units

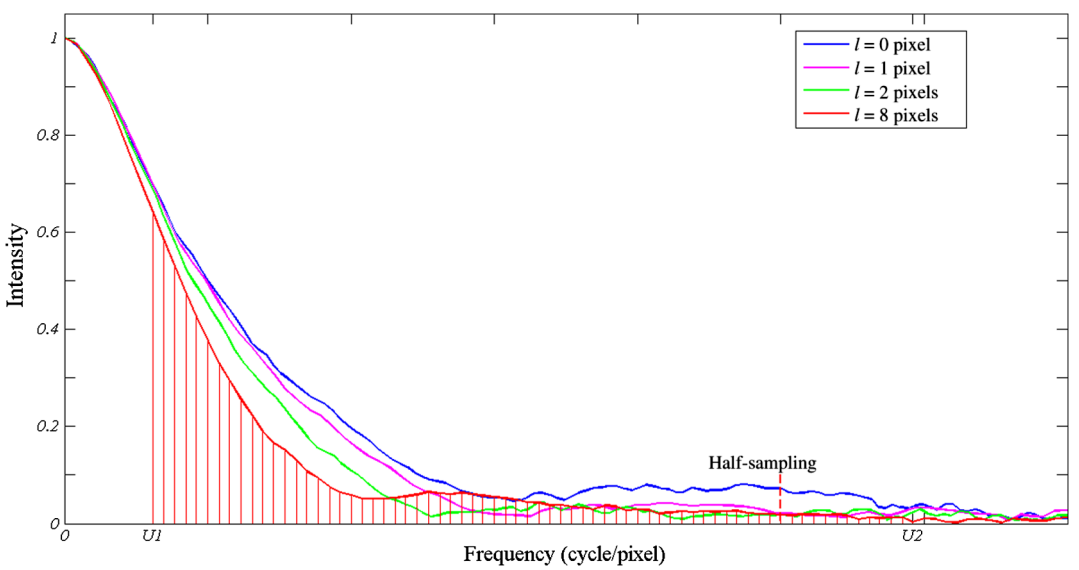

Fig. 3 The comparison of frequency spectrum with l equal to 0, 1, 2, and 8 pixels, respectively.

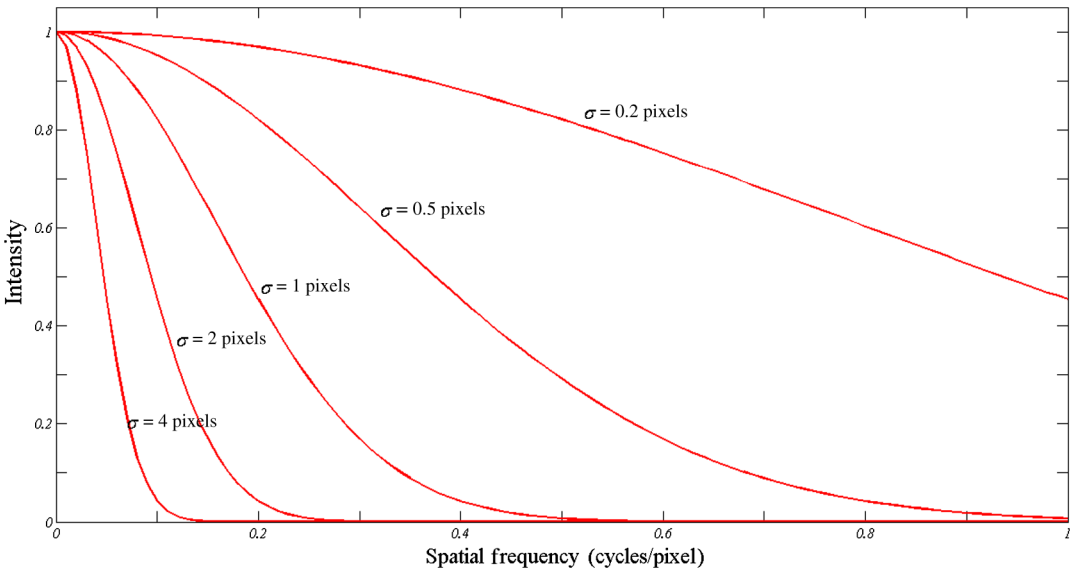

Fig. 4 Gaussian functions with σ equal to 0.2, 0.5, 1, 2, and 4 pixels, respectively.

of pixels. Similarly, the Gaussian function has the characteristic of a low-pass filter. As the image motion increases, high-frequency components are attenuated. Then, the focus measure function decreases due to the effect of Gaussian function. For the images with the same amounts of jitter motion, the decrease of focus measure function is the same for all images. The motion will decrease the maximum of focus measure, but it does not affect the optimal focus position of the system. The position of the peak in the focus measure curve can still reflect the optimal focus position.

3 Analysis of the Influence of Motion on Autofocus

The images suffer from degradation when the image sensor is out of focus. The intensity of the sharpness measure functions varies at different positions. Therefore, the curve of sharpness measure function reflects the autofocus processing. The point in the autofocus curve represents the sharpness of an image. We utilized the difference of focus measures to distinguish the defocus degree of two adjacent images. The difference of focus measure between two images is defined as

$$\Delta F_{\mathrm{DFT}} = \sum_{u=U_1}^{U_2}\sum_{v=V_1}^{V_2} Y_2(u,v) - \sum_{u=U_1}^{U_2}\sum_{v=V_1}^{V_2} Y_1(u,v), \tag{10}$$

where $Y_n(u,v) = |\mathrm{DFT}[y_n(i,j)]|$ is the absolute value of the DFT of an image, and interval of (U_1, U_2) and (V_1, V_2) are the range of high-frequency components.

If the image used for calculating sharpness function suffers from motions, then the focus measure curve will show a small change in the shape. We assume that the two images are convolved with linear shift motions, and the relative distances between the image sensor and object are l_1 and l_2, respectively. Substituting the DFT of the image with motion into Eq. (10), we can obtain the difference of two images that suffer from linear shift motions. To develop a simple analysis of motion, we simplify the Fourier transform results and consider the focus measure functions in 1-D. Then, we can obtain the difference $\Delta F'_{\mathrm{DFT}}$ as

$$\Delta F'_{\mathrm{DFT}} = \sum_{u=\mathrm{U}_1}^{U_2} Y_2(u)\mathrm{sinc}(l_2\cdot u) - \sum_{u=\mathrm{U}_1}^{U_2} Y_1(u)\mathrm{sinc}(l_1\cdot u). \tag{11}$$

If the motion distance in the first image is the same as the second one ($l_1 = l_2$), then it is easy to combine the two terms of Eq. (11) into one and we can obtain

$$\Delta F'_{\mathrm{DFT}} = \sum_{u=\mathrm{U}_1}^{U_2} [Y_2(u) - Y_1(u)]\mathrm{sinc}(l\cdot u). \tag{12}$$

Compared with the autofocus processing without motions, the focus measure curve is substantially modulated by the effect of sinc function. The Fourier frequency components are not changed, but the weight of each frequency component is different. The high-frequency components of sinc function are attenuated, so the difference $\Delta F'_{\mathrm{DFT}}$ is theoretically less than ΔF_{DFT} ($\Delta F'_{\mathrm{DFT}} \le \Delta F_{\mathrm{DFT}}$). The focus measure curve will be attenuated also due to the effect of sinc function. However, the decrease of focus measure will not affect the precision of autofocusing. The maximum value of focus measure is lower, but the peak will not shift. As a conclusion, the optimal focus position reflected by the peak of focus measure curve is accurate. Fig. 5 shows the comparison of several focus measures as a function of detector positions.

In practice, the image motion in the sequences obtained by aerial cameras is not absolutely equal, e.g., $l_1 \neq l_2$. Refer to Eq. (11), the difference of focus measure $\Delta F'_{\mathrm{DFT}}$ can be transformed by adding a couple of virtual terms and simplified as

$$\begin{aligned}\Delta F'_{\mathrm{DFT}} = &\sum_{u=\mathrm{U}_1}^{U_2} [Y_2(u) - Y_1(u)]\mathrm{sinc}(l_2\cdot u) \\ &+ \sum_{u=\mathrm{U}_1}^{U_2} Y_1(u)[\mathrm{sinc}(l_2\cdot u) - \mathrm{sinc}(l_1\cdot u)].\end{aligned} \tag{13}$$

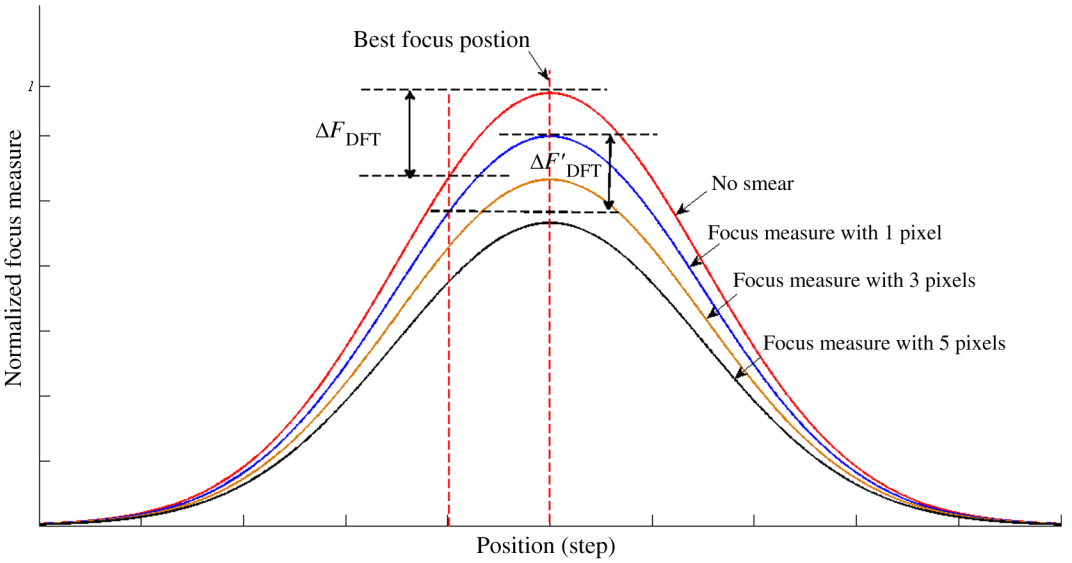

Fig. 5 The focus measure curve with motions compared to that without motions.

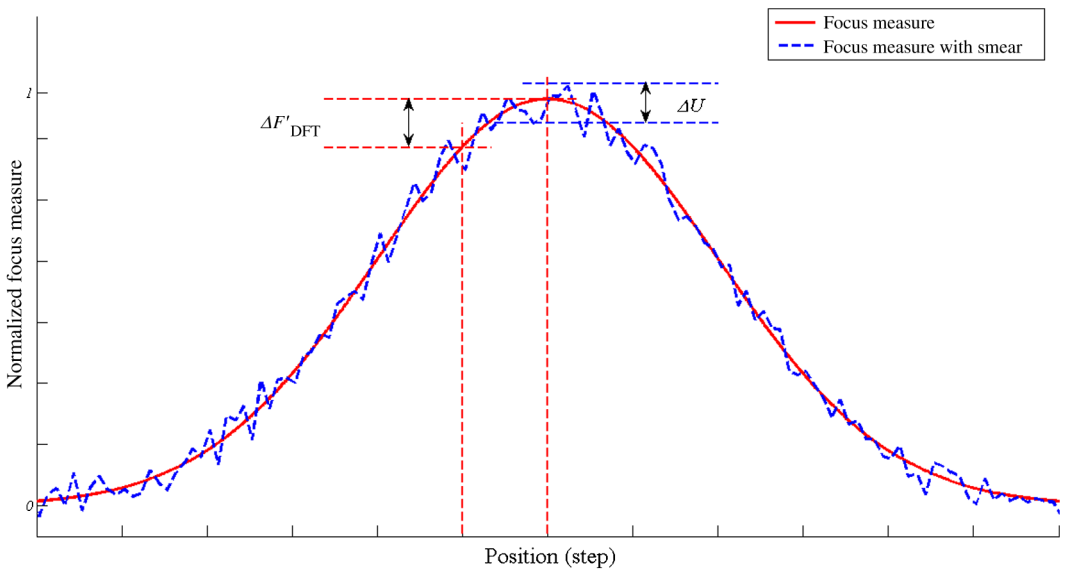

Fig. 6 Focus measure function with motions that change instability.

According to Eq. (13), it is obvious that $\Delta F'_{DFT}$ is correlated with both the degree of blurring and the distance of motion. When the images captured for autofocusing carry different amounts of motions, the focus measure provides poor autofocus precision (as shown in Fig. 6). In other words, when the deviation ΔU caused by unstable motions is larger than the difference of sharpness value of two adjacent images ($\Delta U > \Delta F'_{DFT}$), the motions will begin to affect the autofocus precision. Conversely, if the amounts of motion in two images are approximately equal, the precision will be acceptable.

4 Experimental Results

To further verify the analysis above, a series of experiments were carried out. The autofocus sharpness measure function described in Sec. 2.1 was implemented on a composite imaging system based on a point gray camera and a stepper

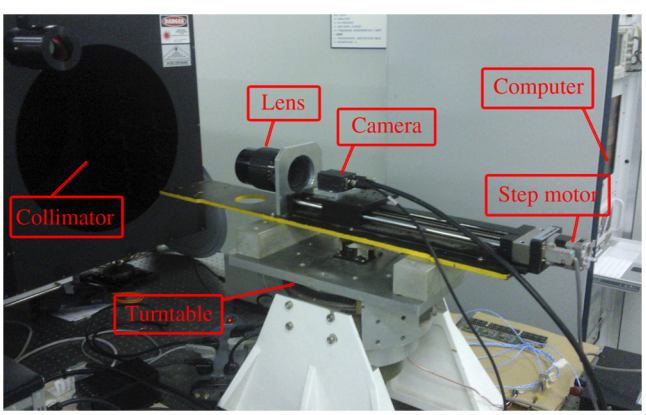

Fig. 7 Structure of the experimental imaging system.

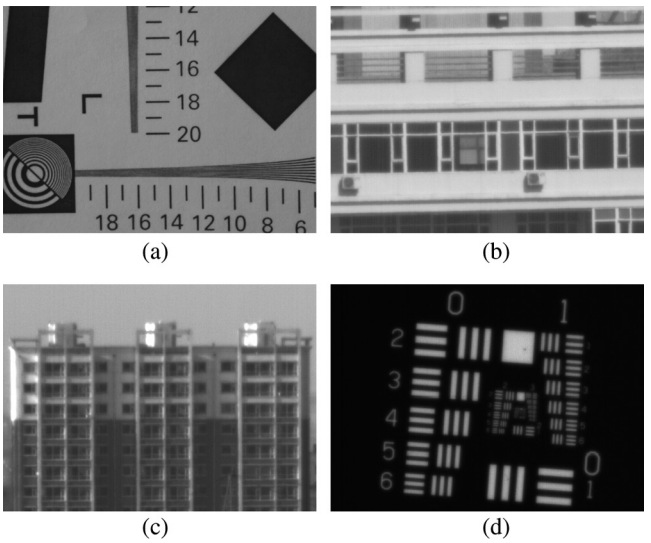

Fig. 8 Four representative scenes: (a) resolution chart (scene distance 2 m), (b) nearby building (scene distance 400 m), (c) far building (scene distance 7000 m), and (d) collimated drone (scene distance infinity).

motor. The detector was driven by the stepper motor, which can move the detector to capture an image at several step positions. The entire imaging system was placed on a horizontal turntable which rotated at a constant speed. The images with different amounts of linear shift motions were captured by adjusting the rotating speed of the turntable. In this section, only the experimental results of linear shift motion images are discussed. Similar observations apply to the jitter motion images. Fig. 7 illustrates the block diagram of the experimental imaging system.

Four representative sequences acquired at the distance from 2 m to infinity were collected. Fig. 8 shows the four scenes as the resolution chart, nearby building, far building, and collimated drone. The distances of scene to lens were 2, 400, 7000, and infinity, respectively.

Four sequences were recorded for each scene with the linear shift motion equal to 0, 1, 3, 5, 8, and 10 pixels, respectively. The frequency spectra-based focus measure was computed for each sequence. A comparison of four autofocus performance was conducted in Fig. 9.

According to Fig. 9, the best focus position is reflected by the maximum value of focus measure. The maximum values

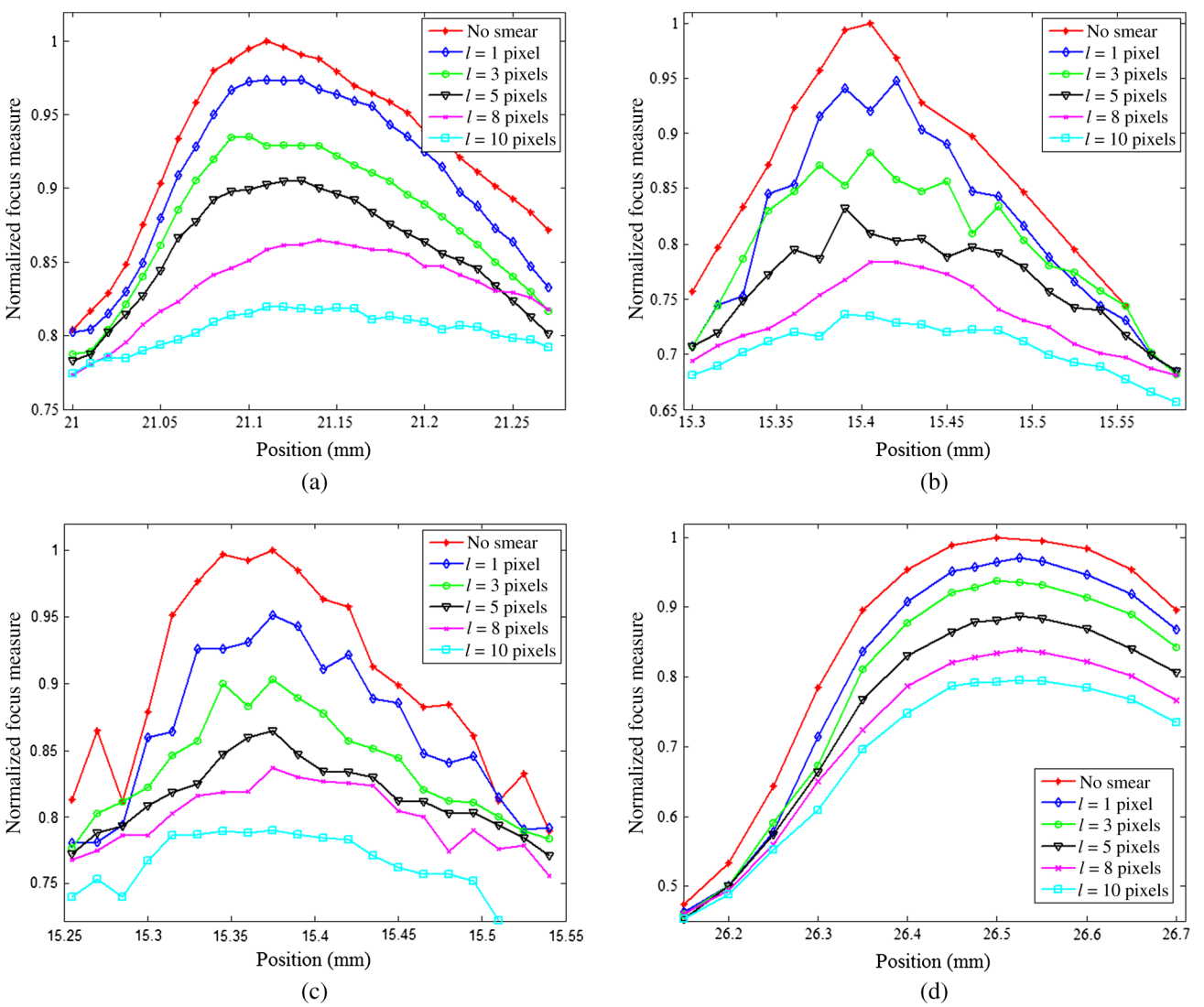

Fig. 9 Autofocus curves based on motion images of four scenes in Fig. 8.

decrease with the increase amounts of image motions. The more motions there are in image sequence, the smaller the maximum in measure functions. The best focus positions of the sequences with motions are close to the one without motion, with only a little shift. It can be seen that the sequences with 8 and 10 pixels motions are so smooth asto have almost no maximum or a peak. The images with motions are similar to the defocus images, then the image-based passive autofocus algorithm can no longer make a distinction between them. It indicates that the autofocus method cannot determine the best focus position. On the other hand, the focus measure curve of the indoor scenes sequences [Figs. 9(a) and 9(d)] are smoother than that of outdoor sequences [Figs. 9(b) and 9(c)] because the outdoor sequences experience more atmospheric turbulence.

To improve the precision of autofocus, the method of quadratic fitting was applied. A smooth curve of autofocus can be attained by fitting a quadratic to these discrete points. The position where the fitted curve reaches a maximum is considered as the focus position. If the image sequences are captured for autofocusing without motions, then the peak of the fitted curve will reflect the focus position. When the images are collected with linear or jitter motions, the quadratic fitted curve minimizes the deviation of all points. Therefore, this method is relatively robust to the image motions. The fitted curve can satisfy the requirement of autofocusing, which can be seen from the quadratic fitted curves of four scenes in Fig. 10.

A comparison of autofocus results is summarized in Table 1. Two conclusions can be drawn from these experimental results. First, the focus measures of image sequences with more amounts of motions will decrease more significantly. For example, the maximum of focus measure for outdoor sequences with 5 pixels are 86.18% and 83.89%, with maximum of focus measure with 10 pixels are 75.55% and 78.91%. The indoor sequences maximum are 91.04% and 88.72% and with 10 pixels are 82.66% and 80.52%. This implies that the outdoors scenes are more sensitive to motions for lack of edge and detailed information. Second, the optimal focus positions of the fitted curves with motions have a little

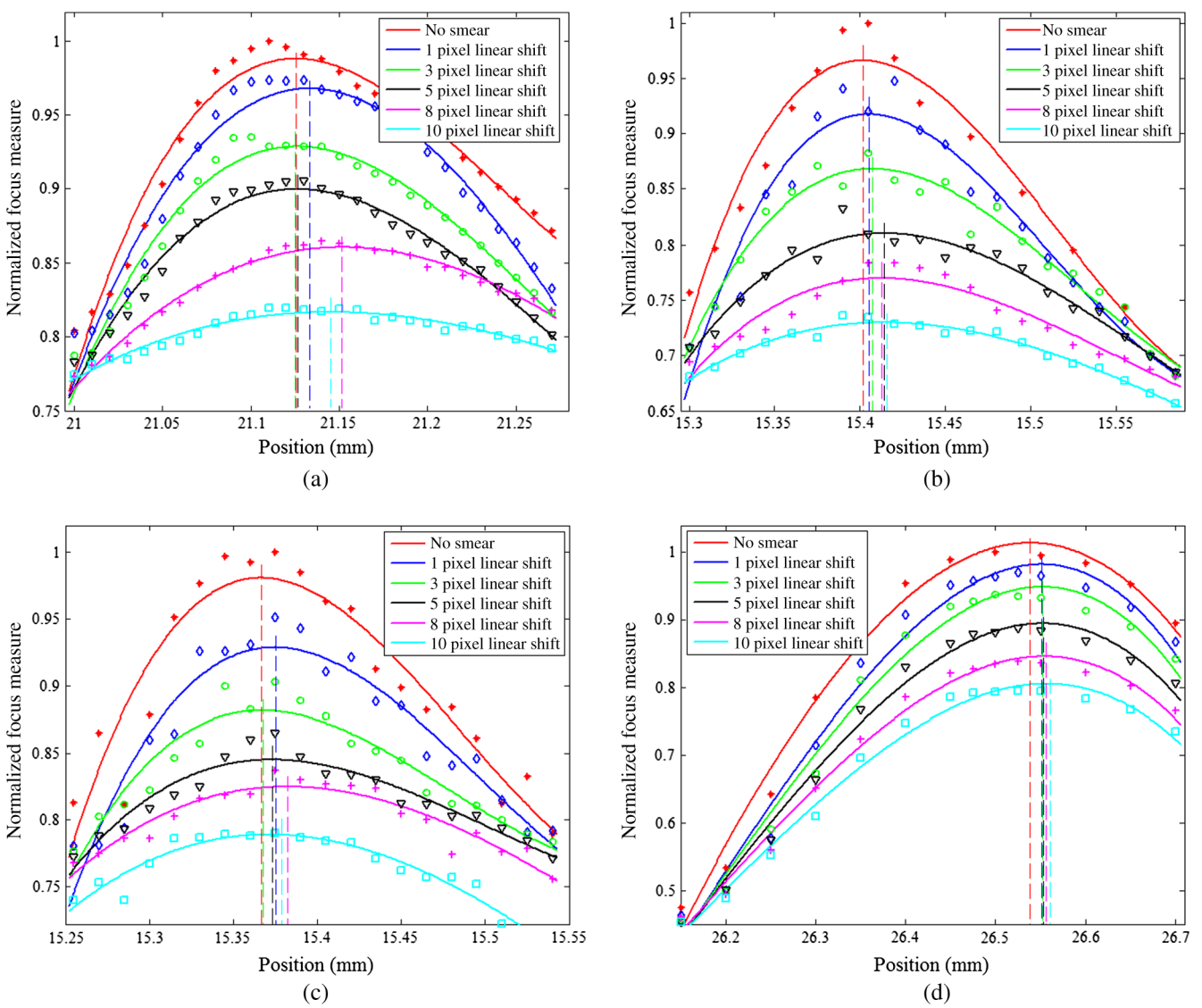

Fig. 10 The quadratic fitted smooth curve of autofocusing in Fig. 9.

Table 1 A comparison of autofocus results.

Objects	Image motion (pixels)	Shift distance (mm)	Decrease of maximum (%)
Resolution chart	0	0	100
	1	0.0078	97.96
	3	0.002	93.97
	5	0.001	91.04
	8	0.0268	87.11
	10	0.02	82.66
Nearby building	0	0	100
	1	0.0035	94.97
	3	0.0058	89.86
	5	0.013	83.89
	8	0.0107	79.69
	10	0.0125	75.55
Far building	0	0	100
	1	0.0083	94.70
	3	0.0001	89.89
	5	0.0064	86.18
	8	0.0155	80.91
	10	0.0042	78.91
Collimator drone	0	0	100
	1	0.012	95.92
	3	0.0125	92.68
	5	0.014	88.72
	8	0.017	84.58
	10	0.028	80.52

shift. The shift distances are shown in the third column of Table 1. In our experiments, the aperture diameter F was 5.6 and the focus length f was 200 mm. The half depth-of-focus can be calculated as

$$\delta = \frac{\Delta}{2} = 2F^2\lambda = 2 \times 5.6^2 \times 0.55 = 0.0345 \text{ (mm)}. \quad (14)$$

A comparison can be presented between the distance and the depth of focus. It is obvious that the shift distances in the third column of Table 1 are smaller than the depth of focus. This means that the optimal focus position of autofocus based on motion images is in the camera's depth of focus. This quadratic fitting technique has the advantage of relative robustness against image motion and works well in autofocus technique. On the other hand, the image sequence with motions can be used for autofocus by fitting a quadratic, and the precision meets the requirement of imaging system.

In practice, the images captured by aerial cameras should be sharp, and it is not allowed to obtain the image with motions beyond three pixels. Therefore, the analysis proposed in this paper is available for aerial cameras.

5 Summary and Conclusions

In this paper, the analysis of the image motion on autofocus precision has been presented for the first time in imaging systems. We concentrated on two image motion models: linear shift motion and jitter motion for autofocusing techniques. The focus measure function based on DFT was applied to evaluate the sharpness of the collected image. We studied and compared the influence of image motion on autofocus precision and the difference of focus measure, and proposed the quadratic fitting method for optimizing the focus position. Experimental results demonstrate that the maximum value of focus measure function decreases more than 10% when the image motion increases to five pixels. The quadratic fitting method meets the requirement of imaging system autofocus. The analysis proposed in this paper was available for aerial cameras.

Acknowledgments

This research was supported by the National Natural Science Foundation of China (No. 61308099).

References

1. Y. Kang et al., "Robust depth-from-defocus for autofocusing in the presence of image shifts," *Proc. SPIE* **7066**, 706609 (2008).
2. M. E. Rudnaya et al., "Orientation identification of the power spectrum," *Opt. Eng.* **50**(10), 103201 (2011).
3. T. Aydin and Y. S. Akgul, "An occlusion insensitive adaptive focus measurement method," *Opt. Express* **18**(13), 14212–14224 (2010).
4. C. M. Chen, C. M. Hong, and H. C. Chuang, "Efficient autofocus algorithm utilizing discrete difference equation prediction model for digital still cameras," *IEEE Trans. Consum. Electron.* **52**(4), 1135–1143 (2006).
5. X. Meng et al., "A method of autofocus for remote sensing camera," *Proc. SPIE* **7813**, 78130L (2010).
6. V. Petrushevsky and A. Guberman, "Application of phase matching autofocus in airborne long-range oblique photography camera," *Proc. SPIE* **9076**, 90760G (2014).
7. Y. Tian, "Autofocus using image phase congruency," *Opt. Express* **19**(1), 261–270 (2011).
8. S. Tao et al., "Wavelet power spectrum-based autofocusing algorithm for time delayed and integration charge coupled device space camera," *Appl. Opt.* **51**(21), 5216–5223 (2012).
9. Y. Wang, Y. Liu, and X.-L. Chen, "A digital autofocusing method based on CCD mosaicing for aerial camera," *Proc. SPIE* **8194**, 81941H (2011).
10. J. Jaehwan et al., "Fully digital autofocusing system with automatic focusing region selection and point spread function estimation," *IEEE Trans. Consum. Electron.* **56**(3), 1204–1210 (2010).
11. Y. Tian, K. Shieh, and C. F. Wildsoet, "Performance of focus measures in the presence of nondefocus aberrations," *J. Opt. Soc. Am. A* **24**(12), B165–B173 (2007).
12. Y. Yao et al., "Evaluation of sharpness measures and search algorithms for the autofocusing of high magnification images," *Proc. SPIE* **6246**, 62460G (2006).
13. S. Yousefi, M. Rahman, and N. Kehtarnavaz, "A new autofocus sharpness function for digital and smart-phone cameras," *IEEE Trans. Consum. Electron.* **57**(3), 1003–1009 (2011).
14. R. D. Fiete, *Modeling the Imaging Chain of Digital Cameras*, SPIE Press, Bellingham, WA (2010).
15. M. Subbarao and J. K. Tyan, "Selecting the optimal focus measure for autofocusing and depth-from-focus," *IEEE Trans. Pattern Anal. Mach. Intell.* **20**(8), 864–870 (1998).
16. R. L. Easton, "Fourier transforms of 1-D functions," in *Fourier Methods in Imaging*, pp. 239–323, John Wiley & Sons, Ltd. (2010).
17. J. Choi et al., "Noise insensitive focus value operator for digital imaging systems," *IEEE Trans. Consum. Electron.* **56**(2), 312–316 (2010).

18. S. L. Smith et al., "Understanding image quality losses due to smear in high-resolution remote sensing imaging systems," *Opt. Eng.* **38**(5), 821–826 (1999).
19. R. D. Fiete and B. D. Paul, "Modeling the optical transfer function in the imaging chain," *Opt. Eng.* **53**(8), 083103 (2014).

Fanhao Meng is a PhD student in the University of the Chinese Academy of Sciences. He received his BS degree in physics from Jilin University in 2011. His current research interests include image processing and autofocus techniques.

Yalin Ding is a senior researcher at Changchun Institute of Optics, Fine Mechanics and Physics, Chinese Academy of Sciences. He has been engaged in research of aerial camera and airborne reconnaissance systems and has been in charge of many major state scientific research projects. His current research interests include aerial camera systems design, and airborne optoelectronic imaging and measurement systems.

Dejiang Wang is a researcher at Changchun Institute of Optics, Fine Mechanics and Physics, Chinese Academy of Sciences. He received his PhD from the University of the Chinese Academy of Sciences in 2013. His current research interests include image motion compensation, aerial camera systems design, and imaging measurement.

Jihong Xiu is a researcher at Changchun Institute of Optics, Fine Mechanics and Physics, Chinese Academy of Sciences. She received her PhD from the University of the Chinese Academy of Sciences in 2005. Her current research interests include signal processing algorithm design and aerial camera image processing and analysis.